



Effects of a large-scale late spring frost on a beech (*Fagus sylvatica* L.) dominated Mediterranean mountain forest derived from the spatio-temporal variations of NDVI

Angelo Nolè¹ · Angelo Rita¹ · Agostino Maria Silvio Ferrara¹ · Marco Borghetti¹

Received: 14 October 2017 / Accepted: 18 July 2018 / Published online: 16 August 2018
© INRA and Springer-Verlag France SAS, part of Springer Nature 2018

Abstract

- **Key message** A remote sensing-based approach was implemented to detect the effect of a late spring frost on beech forests in the Mediterranean mountain region. The analysis of spatio-temporal variability of frost effects on normalised difference vegetation index (NDVI) highlighted the distribution of the canopy damage across the forest according to geomorphic factors such as slope, aspect, and altitude.
- **Context** Increased intensity and frequency of extreme temperatures such as late spring frosts and heat waves represent the main drivers affecting forest ecosystem structure and composition in the Mediterranean region.
- **Aims** The main objective of this study was to evaluate the effects of a late spring frost disturbance, which occurred during spring 2016 in southern Italy, through the assessment of the spatial pattern of the damage to the beech forest canopy associated with the peak decrease in normalised difference vegetation index (NDVI), and the analysis of the NDVI temporal recovery after this frost disturbance.
- **Methods** The forest areas affected by frost were detected through the NDVI differencing technique based on Landsat 8 (OLI/TIRS) imagery time series. The influence of local geomorphic factors (i.e., aspect, elevation, and slope) on forest NDVI patterns was assessed by means of a generalized additive model (GAM).
- **Results** A rather counterintuitive NDVI patterns emerged according to the forest exposition, with NDVI significantly higher on the north facing areas than the southerly ones. The main canopy damage occurred at about 1250 m and reached up to 1500 m asl, representing the altitudinal range affected by the frost disturbance. Finally, the full canopy recovery occurred within 3 months of the frost event.
- **Conclusion** The analysis of seasonal Landsat 8 image time series related to local geomorphic factors, such as aspect, slope, and altitude, and plant phenology on a frost event date, contributed to highlight the NDVI spatio-temporal variation and canopy recovery of a Mediterranean mountain beech forest.

Handling Editor: Barry Alan Gardiner

Contribution of the co-authors A.N. performed all experimental work, ran the data analysis, and wrote the manuscript. A.R. performed data analysis and co-wrote the manuscript. A.F. participated in data interpretation. M.B. supervised the work, participated in results interpretation, and co-worked in paper writing

Electronic supplementary material The online version of this article (<https://doi.org/10.1007/s13595-018-0763-1>) contains supplementary material, which is available to authorized users.

✉ Angelo Nolè
angelo.nole@unibas.it

Angelo Rita
angelo.rita@unibas.it

Agostino Maria Silvio Ferrara
agostino.ferrara@unibas.it

Marco Borghetti
marco.borghetti@unibas.it

¹ Scuola di Scienze Agrarie, Forestali, Alimentari e Ambientali, Università degli Studi della Basilicata, Viale dell'Ateneo Lucano 10, 85100 Potenza, Italy

Keywords Late spring frost · Beech forest · Landsat 8 · Forest disturbance · NDVI differencing

1 Introduction

Changing climate represents the most important threat for mountain forests in the Mediterranean region and affect forests vitality and productivity (Lindner et al. 2014). Although increasing temperatures, atmospheric CO₂ concentration, and nitrogen fertilization suggest an enhancement of plant growth rates at the global scale (Frank et al. 2015; Pan et al. 2011; Xie et al. 2015), the increased frequency of extreme weather events such as spring frosts, heat waves, prolonged drought, and storms (Diffenbaugh et al. 2018; Garcia et al. 2014; Kramer et al. 2000; Williams 2014; Williams et al. 2014) represent the main limitation to forest growth rate especially in the Mediterranean region. Under these ongoing climate changing conditions, Mediterranean forest ecosystems are facing increasing threats related to wildfire risks, pest outbreaks, and forest dieback.

Despite the increasing trend in mean temperatures forecast for all the climate change scenarios (IPCC 2014), extreme events such as spring frosts represent a relevant climatic stress factor for mountain vegetation in the Mediterranean region, due to increases in daily temperature variance characterizing the ongoing climatic change (Gu et al. 2008; Nicholls and Alexander 2007; Pagter and Arora 2013; Rigby and Porporato 2008; Vitasse et al. 2018; Wang et al. 2014).

Warmer winters and spring temperatures affect plant phenology because the predicted opening of vegetation buds and leaf expansion increases plant vulnerability to late spring frosts (Augsburger 2013). According to Jeong et al. (2011), European forests showed an early start of the growing season by 3.5 days decade⁻¹ and a total increase of the growing season by 6.5 days decade⁻¹.

These extreme events according to their magnitude, frequency, and spatial scale may affect not only forest productivity but also species composition and distribution with important consequences at an ecosystem level. Nevertheless, most of these events are not taken into account because of their small spatial scale, but their frequency combined with their distribution at a local scale and their effects distributed over several growing seasons, represent a key driver of forest productivity loss and a carbon uptake reduction unaccounted for the ecosystem level (Bascietto et al. 2018; Hufkens et al. 2012; Kim et al. 2014; Príncipe et al. 2017).

The main impacts of spring frosts are related to foliar mortality due to ice formation within buds and leaf cells and tissues. Frost damages at a higher intensity may affect apical meristems causing changes in the canopy architecture with a generalized reduction in tree productivity due to late refoliation from branch and epicormic dormant or

adventitious buds (Augsburger 2009; Dittmar et al. 2006; Kramer and Kozłowski 1979; Vitasse et al. 2014).

Mountain forests in the Mediterranean region are particularly exposed to frost disturbance due to the combination of anticipation of phenological phases induced by warmer late winter temperatures and spring frost events. In particular, beech forests (*Fagus sylvatica* L.), widely distributed in Europe from the southern latitudinal limit in Sicily up to the northern latitudinal limit in south Norway, show a higher sensitivity to late spring frost than other forest species (Kreyling et al. 2012; Príncipe et al. 2017). In the Mediterranean region, beech forests represent the climax forests, growing at higher altitudes from 900 to 1000 m asl up to the vegetation limit (Houston et al. 2016). In the last two decades, beech forests at the southern limit are experiencing long-term drought stress related to climate change, limiting forest productivity, and at the same time shaping the lower altitudinal population limit (Jump et al. 2006). Moreover, the phenological phase anticipation induced by warmer late winter temperatures of southern beech populations, with respect to Central and South-East European populations, as observed by Visnjic and Dohrenbusch (2004), makes Mediterranean populations more exposed to spring frost events.

Detecting the spatial distribution of these disturbances and the recovery patterns of forest vegetation cover, represent key information for forest management and forest productivity analysis and modeling in order to make reliable estimates of carbon uptake at the regional scale. In the last few decades, Landsat satellites (Landsat 2, 3, 4, 5, and 7) have provided near-global moderate-resolution imagery based on multispectral scanners. Landsat images have been used by the scientific community for ecosystem level monitoring, including the management and analysis of agriculture and forest, and land cover change assessment (Roy et al. 2014). Since 2013, the new Landsat 8 satellite, equipped with the new sensors Operational Land Imager (OLI) and the Thermal Infrared Sensor (TIRS), provides imagery with refined bands designed to operate in continuity with Landsat TM and ETM+ and two bands in the region of the thermal infrared, for a better characterization of land and vegetation cover. Landsat TM, ETM+, and Landsat 8 time series have been used to detect on a small scale growing season phenology up to large-scale vegetation changes based on the normalized difference vegetation index (NDVI) detection change (Cohen and Fiorella 1998; Coppin et al. 2004; Hayes and Sader 2001; Kovalsky et al. 2012; Lu et al. 2004; Mancino et al. 2014; Pasquarella et al. 2016). Being NDVI anomalies related to sudden changes of several biotic (e.g., pests) and abiotic (e.g., drought stress, flooding, and geomorphological processes) agents, the spatio-

temporal analysis of NDVI pattern based on satellite image time series, may help to detect the impact of known short-term extreme weather events such as spring frosts.

In this study, we analyze the effects of a regional scale spring frost disturbance, which occurred during April 2016 in southern Italy, using 16-day Landsat 8 (OLI/TIRS) time series covering the 2016 growing season. In particular, we investigate the possibility of identifying frost disturbance legacies on forest canopy cover at the end of the growing season, and to analyze spatial variability of late spring frost damages on beech forests based on remote sensing analysis.

Thus, the main objectives of the present study are (i) to assess the spatial pattern of the damage to a beech forest canopy due to a late spring frost and correlated with the peak decrease of NDVI and (ii) to analyze the NDVI temporal recovery after this late spring frost.

2 Materials and methods

2.1 Study area and frost event

The study area is represented by the beech forests covering the Apennine Mountain range of the Basilicata Region in southern Italy. The geomorphology of the region is mostly characterized by mountainous terrain covering almost 90% of its area. The main mountain range is represented by the Apennine Mountains in the eastern part of the region (46.8%), (Online Resource1/OR1) containing the highest peaks of the southern Apennine range, reaching 2248 m asl at Monte Pollino. The western part of the region is mainly characterized by low hills (45.2%) with an altitude below 600 m, sloping towards flat plains on the south coast, along the Ionian Sea.

The climate is consistent with the topographic variability of the region, alternating between a Mediterranean humid type in the mountain area and a Mediterranean dry type in the western part of the region (Mancino et al. 2014). According to the Basilicata Region Forest Atlas (Costantini et al. 2006) (OR1), beech forests occupy 29,900 ha, representing 8.5% of the total regional forests and distributed up to the vegetation limit (1900–2000 m asl).

The late spring frost event studied in this paper was a fast cold air mass with north easterly winds, which occurred on the 25th and 26th of April 2016 (DOY 116/117). Sub-freezing temperatures occurred above 900–1000 m asl, with minimum temperatures reaching -5.63 °C on DOY 116, as derived from the MODIS/Terra Land Surface Temperature and Emissivity (LST/E) Daily L3 Global 1-km Grid product (MOD11A1) (Fig. 1). Measured daily minimum temperatures were selected according to local meteorological stations closest to the study area (ALSIA Regional Agency, <http://www.alsia.it/opencms/opencms/Servizio/SAL/rete.html>). The

Online Resources (OR2) provided in supplementary material clearly shows the drop of temperatures on the 25th and 26th of April 2016. The frost event severely damaged green leaves within an irregular altitudinal range along the beech forest distribution, depending on the combination between local geomorphic variables like slope and aspect and plant phenology. The low limit of the frost-affected area was determined by the altitude of sub-freezing temperatures, while the upper limit was determined by the plant phenology characterized by unfolded leaves on that date. As a consequence of this combination, the entire slope of the Apennine mountain range turned brown producing a “burned band” persistent during most of the vegetative season (Fig. 2).

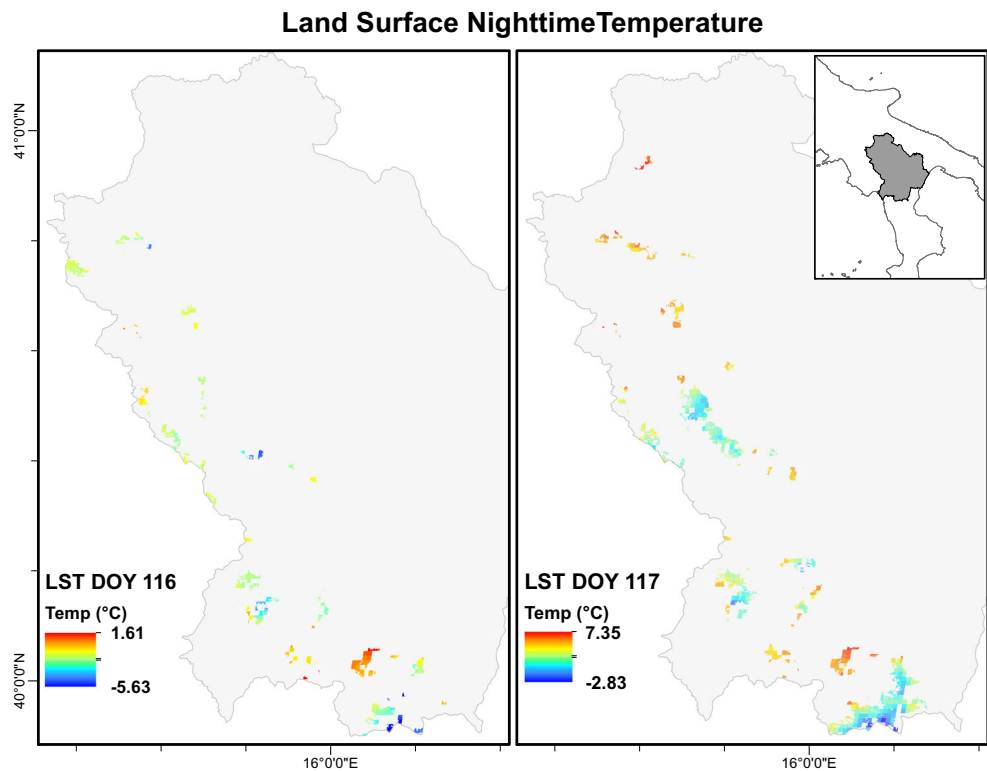
2.2 Landsat 8 OLI/TIRS data and image pre-processing

To assess the extension of beech forest areas affected by the frost disturbance and analyze the NDVI variability across a geographic range, we used 16-day orthorectified and terrain-corrected collection 1 level 1 Landsat 8 OLI/TIRS images (Table 1). The images were downloaded from the USGS EarthExplorer website (<https://earthexplorer.usgs.gov/>), and registered with UTM coordinates, Datum WGS84, Zone 33 N (path = 188; row = 32). The quality of the images was assessed from Landsat 8 OLI quality assessment (QA) band, by masking contaminated pixels (clouds, cloud shadows, cirrus, and water) using a cloud masking Qgis plugin (Corredor 2018). All images were radiometrically calibrated in order to convert the quantified energy expressed in digital numbers (DN) into at-sensor radiance. Then, images were corrected to top-of-atmosphere (TOA) reflectance which is the planetary reflectance corrected by incorporating exo-atmospheric solar irradiance, Earth–Sun distance, and solar elevation angle at the image acquisition, provided by the associated metadata file (MTL). Finally, all the images were atmospherically corrected using the atmospheric correction algorithm Fast Line-of-sight Atmospheric Analysis of Spectral Hypercubes (FLAASH), based on MODTRAN4 radiative transfer code (Felde et al. 2003). The model was parameterized according to the FLAASH user’s manual for multispectral imagery (ENVI 2009). For all the corrected images, the NDVI was calculated using the following Eq. 1, where ρ_{RED} and ρ_{NIR} are band 4 (red, 0.64–0.67 μm) and band 5 (near-infrared, 0.85–0.88 μm) reflectance respectively.

$$\text{NDVI} = \frac{\rho_{\text{NIR}} - \rho_{\text{RED}}}{\rho_{\text{NIR}} + \rho_{\text{RED}}} \quad (1)$$

Finally, NDVI images were clipped to the area covered by beech forests according to the forest class distribution of the Basilicata Region Forest Atlas (Costantini et al. 2006).

Fig. 1 MODIS/Terra Land Surface Temperature and Emissivity (LST/E) Daily L3 Global 1-km Grid product (MOD11A1) for DOY 116 (left panel) and 117 (right panel) 2016



2.3 NDVI differencing

In order to identify frost disturbance legacies on forest canopy cover after seasonal NDVI recovery, and thus to identify the extension of beech forests affected by late spring frost, we implemented the NDVI differencing technique (Lunetta et al. 2006; Lyon et al. 1998; Nabuurs et al. 2007; Podeh et al. 2009; Schowengerdt 1997; Wilson and Sader 2002). This technique is based on the change detection analysis between two NDVI images and identifies the pixels representing significant positive and negative changes in the tails of a normal distribution of a NDVI difference image histogram. On the contrary, the pixels with no significant changes are clustered around the mean. The NDVI difference image (hereafter Δ NDVI) was then calculated as the difference between the



Fig. 2 The “burned band effect” of late spring frost event over beech forest in the Pollino National Park area (a). Detailed picture of the event in the same area at 1600 m asl taken in June 2016 (b)

Table 1 16-day Landsat 8 scenes for 2015 and 2016 growing season

Date	DOY
13 August 2015	225
27 May 2016	148
12 June 2016	164
28 June 2016	180
14 July 2016	196
30 July 2016	212
15 August 2016	228
31 August 2016	244
16 September 2016	260

Landsat 8 retrieved NDVI values on the 15th August 2016 (DOY 228) and the value on the 13th August 2015 (DOY 225) (Fig. 3). The ΔNDVI was then reclassified using a threshold value calculated as $(\mu - n \times \sigma)$; where μ represents the ΔNDVI pixels mean, σ is the ΔNDVI pixels standard deviation, and n represents the threshold value. The threshold identifies the values of $\Delta\text{NDVI} < (\mu - n \times \sigma)$ representing the pixels characterized by a significant change in NDVI from 1 year to another due to the frost effects. In order to identify the best fit of $n \times \sigma$ to the average ΔNDVI , the n value was calibrated through the trial and test approach, by comparing different n values ($n = 0.6$, $n = 1$, and $n = 1.5$) against ground-truth control points. To this purpose, between May and June 2016, we walked through the forest and selected 21 sites where the canopy appeared heavily affected by frost damage, and 15 sites where the canopy appeared totally unaffected. For each site, we geo-referenced a control point and we used them for the assessment of the best fitting of $n \times \sigma$ of the NDVI difference image average. The complete list of ground-truth control points is now provided in the Online Resources (OR3). Finally, the best fit of $n \times \sigma$ thresholds was determined by Cohen's Kappa inter-rater agreement coefficient, which identified $n = 1$ (OR4).

2.4 NDVI spatio-temporal variability analysis

In order to analyze the effects of the frost disturbance on beech forest NDVI variability on a regional scale, we analyzed the 2016 growing season using 16-day time step calculated NDVI related to local geographical variables. In particular, we used the information derived from the 20-m digital terrain model (Ministero dell'Ambiente e della Tutela del Territorio e del Mare 2012) to calculate elevation slope and aspect for the study area. The geographic and temporal relationships between the dependent (NDVI) and the independent variables (DOY as time, elevation, and slope) were investigated via generalized additive models (GAMs) (Hastie and Tibshirani

1990). GAMs are a non-parametric extension of the generalized linear model (GLM) allowing the inclusion of a non-parametric smoothing function and thus fitting a nonlinear relation among variables. Further, the "aspect" term (dummy coded as North 270° to 90° and South 90° to 270°) was included in the model as a grouping factor, and a tensor product function (i.e., an anisotropic interaction term between x and y) was used both for latitude and longitude and elevation and slope to account for the spatial and geomorphic interactions, respectively. The level of complexity (nonlinearity) of model terms was determined by the estimated degrees of freedom (e.d.f.) of the smoother by using the generalized cross-validation (GCV) criterion, which measures the predictive-squared error of the model (Wood 2006), with low GCV values representing the best compromise between model complexity and fit to the observed data. The contribution of each predictor was assessed by comparing simpler against complex models by the Chi-square likelihood ratio tests. The Wald statistics tested the significant difference of smooth terms from null functions. Finally, the implementation of a specific autocorrelation structure AR(1) in the model accounted for temporal residual autocorrelation.

Data availability The dataset generated and analyzed during the current study is available in the Figshare repository, <https://doi.org/30410.6084/m9.figshare.6409235.v1>. (Nolè et al. 2018). Datasets not peer-reviewed.

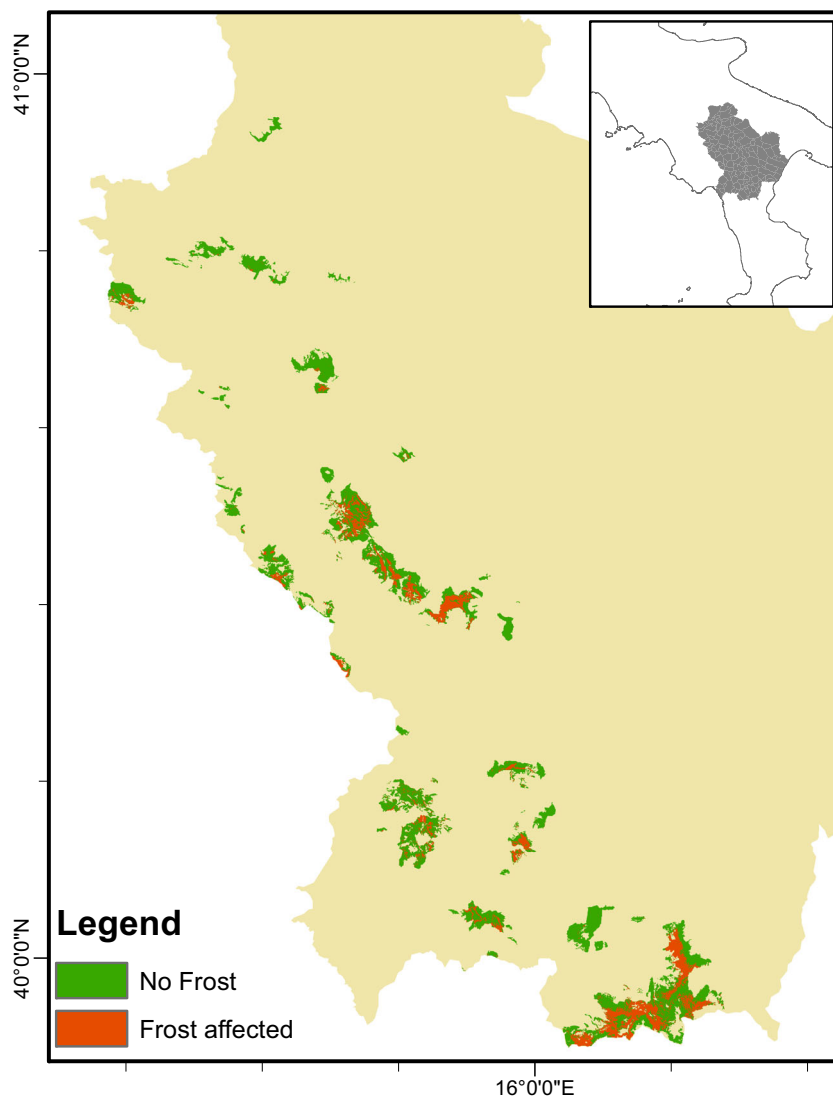
3 Results

The implementation of the NDVI differencing technique provided a detailed map, at a 30-m spatial resolution, of the beech forest affected by the frost disturbance, based on the NDVI differences at the end of the growing season (Fig. 4). The area affected by frost disturbance, calibrated against ground-truth control points, was obtained using a threshold of $1.0 \times \sigma$ ($n =$

Fig. 3 Landsat 8 bands composition (4, 3, 2) (path = 188; row = 32) for the 13th of August 2015 (DOY 225) and the 15th of August 2016 (DOY 228)



Fig. 4 Distribution of the beech forest areas affected and unaffected by the frost event



1) that showed the best accuracy between the different n values tested ($n = 0.6$, $n = 1$, and $n = 1.5$) (OR4).

The frost affected areas, identified with $\Delta\text{NDVI} < (\mu - 1 \times \sigma)$, cover about 13% (3887.26 ha) of the total regional beech forests (29,902 ha), distributed along a 400-m altitudinal range with a mean altitude of 1440 m asl. Figure 5a shows the difference between the average NDVI values of frost affected and frost unaffected beech forests during the vegetative season. An almost full recovery of average NDVI values between the two forest areas is reached at mid-July (DOY 196). During the rest of the vegetative season (DOY 212, 228, 244, 260), the average NDVI seasonal pattern for frost affected and unaffected beech forests constantly shows a slight difference.

Figure 5 shows the seasonal patterns of average NDVI for each Landsat 8 scene (DOY 148 to 228) calculated at 25-m altitudinal steps. The NDVI vs elevation seasonal patterns clearly show the NDVI drop and recovery for each DOY

and highlight that most of the canopy recovery occurs between the end of June and the end of July (DOY 180–212). Furthermore, the NDVI vs elevation patterns at DOY 212 and 228, show lower NDVI values between 1000 m asl and 1750 m asl, than the values at higher altitudes above 1750 m, which are usually lower during an undisturbed growing season. This seasonal pattern shows that the frost event actually affected a wide altitudinal range and thus there was a lower altitudinal limit of the frost affected area compared to that detected by the NDVI differencing technique referring to the mid-August NDVI. This difference in the results is due to the NDVI differencing calibration based on visual observations using ground-truth control points only in stands with canopies heavily affected by frost damages.

The spatial distribution of frost affected area, based on terrain aspect, shows a higher distribution of the forest areas facing North-West to North-East (Fig. 6), accounting for approximately 63% of the total frost affected beech forests.

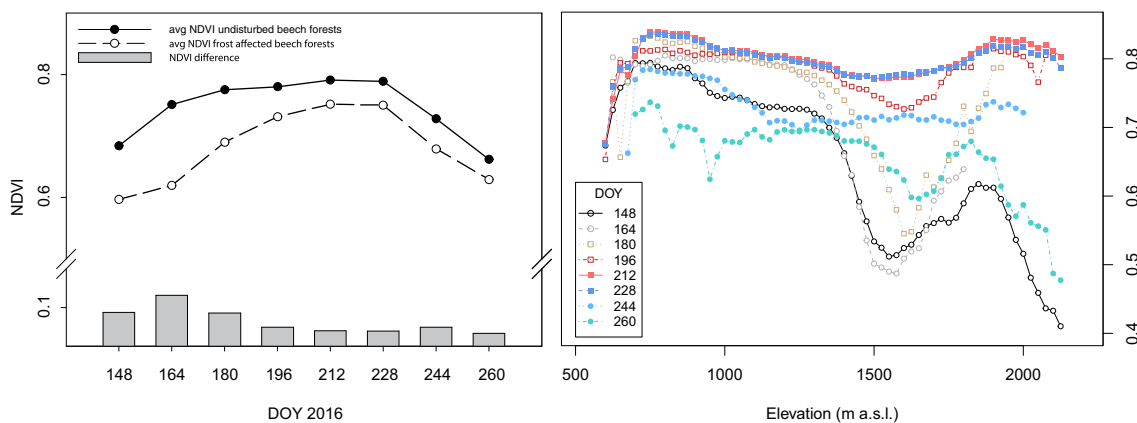


Fig. 5 Seasonal patterns of average NDVI (disturbed and undisturbed) and NDVI differences for growing seasons 2016 (DOY 148, 164, 180, 196, 212, 228, 244, 260) (left panel). Altitudinal patterns of average NDVI at 25-m altitudinal steps during the 2016 growing season (right panel)

Based on this distribution, a generalized additive model was applied to evaluate the spatio-temporal NDVI variability according to northerly and southerly expositions (Table 2 and Fig. 7) which accounts for more than 47% of the explained deviance. The most appreciable relationship detected by the model shows an NDVI increasing trend during the vegetative season up to the maximum values reached in mid-August. Interestingly, the NDVI values are significantly higher on the northerly slope than on the southerly one, and thus suggesting a higher impact of the frost disturbance over the beech forests facing south. The same differences between both expositions are also evident by examining the slope influence on NDVI pattern. A rather distinct picture emerges from GAMs

highlighting a clear relationship between NDVI and elevation, where the frost disturbance “footprint” can be observed along the altitudinal range through an evident decrease in NDVI values. In particular, the main NDVI decrease occurs from about 1250 m and peaks at 1500 m asl, representing the altitudinal range affected by frost disturbance, with constant positive differences between north and south facing forest NDVI. However, the relation showed a different pattern between northerly and southerly expositions, with the southerly NDVI presenting a first drop at lower altitudes than the northerly one. Although the North and South facing patterns appear quite similar, the forest NDVI estimates differences (Fig. 7f) below 1000 m asl and between 1700 and 1900 m asl, show

Frost affected area (%) vs aspect distribution

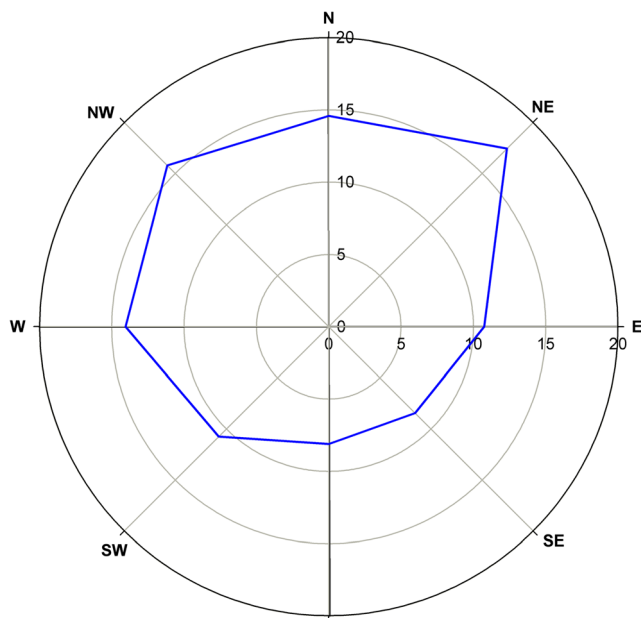


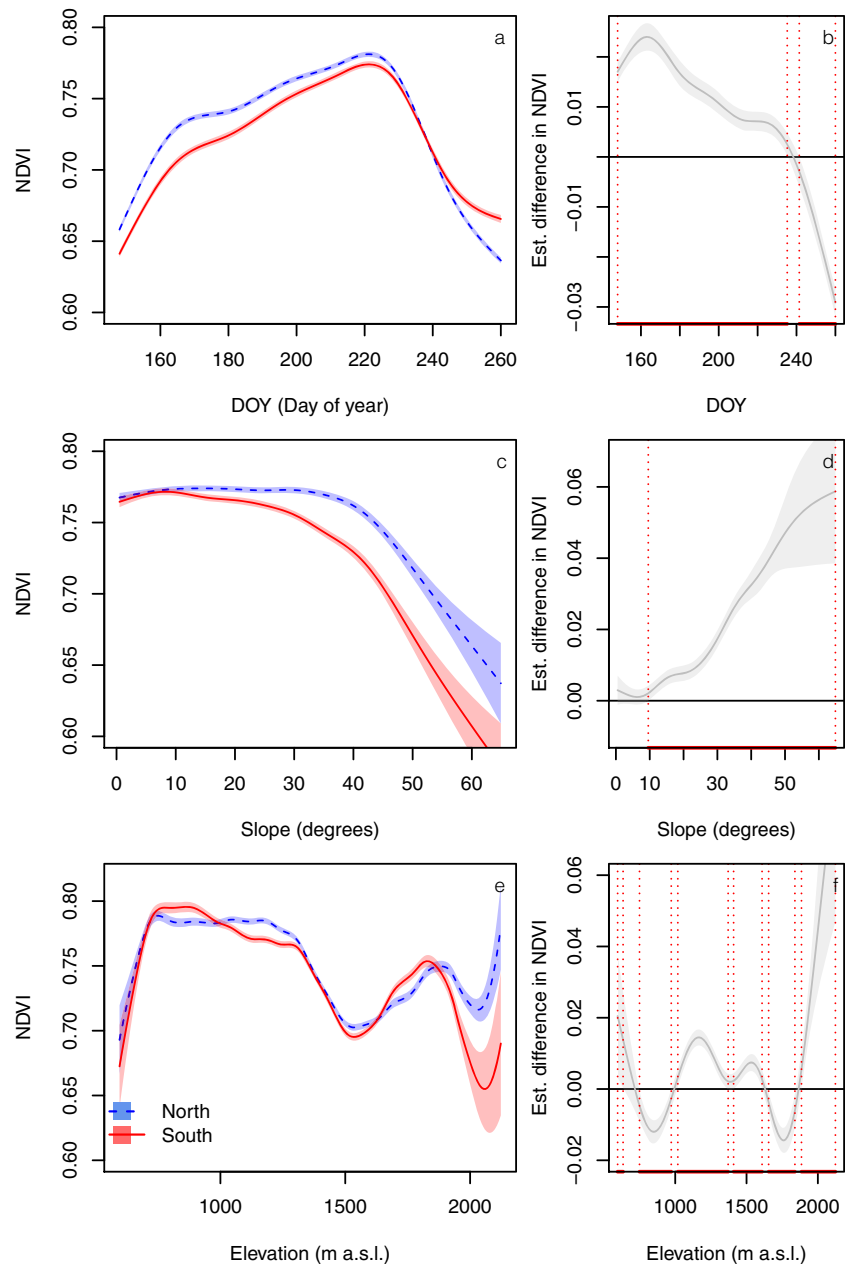
Fig. 6 Percent distribution of frost affected beech forest compared with site aspect

Table 2 Model summary for the generalized additive models fitted to the NDVI

Parametric coefficients	Estimate	Std. error	<i>t</i> value	<i>p</i> value
(Intercept)	0.7447	0.0002	4013.3921	***
S	-0.0073	0.0002	-35.3880	***
Smooth terms	e.d.f	Ref. df	<i>F</i> value	
<i>s</i> (DOY):N	6.9912	7.0000	10,051.2940	***
<i>s</i> (DOY):S	6.9849	6.9999	6420.2012	***
<i>s</i> (elevation):N	8.7029	8.9142	23.6298	***
<i>s</i> (elevation):S	7.6982	7.9130	26.5539	***
<i>s</i> (slope):N	8.3733	8.8512	78.3521	***
<i>s</i> (slope):S	7.3191	7.8172	109.9655	***
<i>ti</i> (elevation, slope)	23.0049	23.6645	34.5531	***
<i>ti</i> (lat,lon)	23.9245	23.9995	736.6596	***

The approximate significance of smooth terms *s* is reported, with the effective degrees of freedom (e.d.f.), referenced degrees of freedom (Ref. df) used to compute the *p* value, and *F* statistics. Symbols are as follows: *N*, north exposition; *S*, south exposition; *lat*, latitude; *lon*, longitude; *s*, thin plate regression spline; *te*, tensor product function; *** indicate significance at *p* < 0.001. The greater the estimated degrees of freedom (e.d.f.), the more the smooth invests in wiggleness

Fig. 7 Predicted smoothing curve (left panels) of NDVI and DOY, slope, and elevation variables assessed using generalized additive model (GAM). Full and dashed lines represent northerly and southerly exposition classes. The shaded areas indicate the 95% confidence interval. In these plots, a positive slope of the line shows a positive effect of the x variable, and a negative slope of the line indicates a negative effect. Right panels shows the estimated difference between the two conditions, i.e., north and south exposition. Bounding vertical dotted lines identify statistical differences detected by performing simultaneous 95% confidence intervals around the estimates



NDVI values following their natural pattern with the southerly forest NDVI higher than the northerly one.

4 Discussion

The study of the effects of the regional scale late spring frost on Mediterranean beech forests showed an effective approach for the spatio-temporal variability detection of frost disturbance and a detailed description of the remote sensing retrieved NDVI patterns (White et al. 2014). The NDVI differencing technique has been mainly used for the detection of forest vegetation changes and disturbances (Zhang et al.

2003, 2004). In this case study, we used the NDVI differencing technique in order to identify the area affected by frost damages and presenting at the end of the growing season the disturbance legacies on forest canopy NDVI.

The calibration of the threshold through the trial and test approach, based on ground-truth control points, confirmed the reliability of the methodology to identify significant differences between the NDVI calculated for mid-August of the 2 years 2016 and 2015 (Pu et al. 2008).

The frost-affected NDVI patterns observed during the 2016 vegetative season suggest a second leaf unfolding starting from the end of June (DOY 180) after almost a 2-month delay, and then completed at the end of July (DOY 212). The second

leaf unfolding required about 30 days for the complete NDVI recovery. As shown by Menzel et al. (2015), this period of time is consistent with the observations found in central European beech forests. However, it is worth noting that the delay between the frost event and the second leaf unfolding is double that of Menzel et al. (2015). This delay is probably due to the severity of the frost event (Hufkens et al. 2012) reaching at higher elevations temperatures far below $-3\text{ }^{\circ}\text{C}$ which is considered the threshold for permanent leaf damage (Dittmar et al. 2006; Sakai and Larcher 1987).

Results from GAM highlighted significant influence of slope, altitude, and aspect on NDVI values where a clear distinct pattern between northerly and southerly exposure emerged. The low NDVI values in forest stands facing south, distributed from about 1000 to 1600 m asl, might be considered as a consequence of the high phenotypic plasticity characterizing the phenological shift of beech populations, according to both elevation and exposition (Vitasse et al. 2010). Moreover, the north-facing beech forest canopies might be characterized by an incomplete bud flush at the moment of the frost event, preserving more buds from frost damage.

A complex NDVI pattern related to elevation represents an interesting result of our analysis, showing independent patterns between northerly and southerly forest exposure. The double drop in the southerly NDVI curve can be interpreted according to the level of canopy browning. The first one, which occurred around 1000 m asl, may suggest a partial canopy frost damage. The second drop, with north/south NDVI curves overlapping each other, may correspond to the forest altitudinal belt which was completely affected by frost disturbance as also highlighted by the NDVI differencing. The lower altitude beech population experienced non-lethal temperatures that contributed to reduced damages at the canopy level but still gave slightly lower NDVI values than the unaffected beech forest observed at full canopy recovery.

Although beech forests are characterized by a high resilience in growth capacity in response to late spring frost (Principe et al. 2017), the combination of subsequent extreme events may dramatically reduce the species resilience. Considering the forest NDVI as a proxy of forest productivity, the effects of spring frost may have a negative impact on forest carbon uptake due to defoliation. The observed reduction of NDVI and the shortening of the growing season may reduce forest productivity by 7–14%, as recently reported by Bascietto et al. (2018) and by Principe et al. (2017). Furthermore, a secondary bud flush during the same growing season causes a depletion of plant carbon reserve. Thus, in the context of the mountainous Mediterranean region, the increasing frequency and duration of extreme events, as was the case with the spring frost of 2016 followed by the summer heat wave of 2017 (Di Giuseppe et al. 2017), can further reduce forest productivity and affect the species resilience at the same time.

5 Conclusion

The 2016 late spring frost event provided an opportunity to explore Mediterranean mountain beech forest sensitivity and recovery patterns to frost disturbance through the spatio-temporal analysis of forest NDVI. The implementation of the NDVI differencing technique based on Landsat 8 images allowed the identification of the spatial distribution of the frost disturbance on the forest canopy by the detection of a persistent reduction of forest canopy NDVI at the end of the growing season. About 13% of the total regional beech forests, distributed across a 400 m altitudinal range, had canopies damaged by this late spring frost. The main results also highlighted the significant influence of topographic variability on NDVI values with a distinct pattern between northerly and southerly exposure emerging due to the marked differences in the phenological stage of these trees when the frost occurred. Then, after a 2-month lag in leaf unfolding, the full canopy recovery of the affected areas took about 30 days based on the NDVI pattern analysis. The results of this study represent a contribution to the better understanding of Mediterranean beech forest sensitivity to the increasing threats of extreme events under changing climatic conditions.

Acknowledgements Landsat 8 OLI/TIRS images courtesy of the U.S. Geological Survey. The authors also acknowledge Pasquale Larocca for granting the use of the photo in Fig. 2.

Funding This work was supported financially by the MIUR-PRIN “CARBOTREES” [grant number 201049EXTW_008] and by the Pollino National Park, Rotonda, Italy, in the framework of the project “Un laboratorio naturale permanente nel Parco Nazionale del Pollino.”

Compliance with ethical standards

Conflict of interest The authors declare that they have no conflict of interest.

References

- Augsburger CK (2009) Spring 2007 warmth and frost: phenology, damage and refoliation in a temperate deciduous forest. *Funct Ecol* 23: 1031–1039. <https://doi.org/10.1111/j.1365-2435.2009.01587.x>
- Augsburger CK (2013) Reconstructing patterns of temperature, phenology, and frost damage over 124 years: spring damage risk is increasing. *Ecology* 94:41–50
- Bascietto M, Bajocco S, Mazzenga F, Matteucci G (2018) Assessing spring frost effects on beech forests in central Apennines from remotely-sensed data. *Agric For Meteorol* 248:240–250. <https://doi.org/10.1016/j.agrformet.2017.10.007>
- Cohen WB, Fiorella M (1998) Comparison of methods for detecting conifer forest change with thematic mapper imagery. In: Lunetta RS, Elvidge CD (eds) Remote sensing change detection, environmental monitoring methods and applications. Ann Arbor Press, Chelsea, pp 89–102
- Coppin P, Jonckheere I, Nackaerts K, Muys B, Lambin E (2004) Digital change detection methods in ecosystem monitoring: a review. *Int J*

- Remote Sens 25:1565–1596. <https://doi.org/10.1080/0143116031000101675>
- Corredor X (2018) CloudMasking Qgis plugin (version 18.2.7), SMBYC-IDEAM and FAO. Available: <https://smbyc.bitbucket.io/qgisplugins/cloudmasking>
- Costantini G, Bellotti A, Mancino G, Borghetti M, Ferrara A (2006) Carta forestale della Basilicata - Atlante. INEA - Regione Basilicata, Potenza, p 99 ISBN 88-8145-062-3
- Diffenbaugh NS, Singh D, Mankin JS (2018) Unprecedented climate events: historical changes, aspirational targets, and national commitments. *Sci Adv* 4:eaa03354. <https://doi.org/10.1126/sciadv.aao3354>
- Dittmar C, Fricke W, Elling W (2006) Impact of late frost events on radial growth of common beech (*Fagus sylvatica* L.) in Southern Germany. *J Forest Res* 125:249. <https://doi.org/10.1007/s10342-005-0098-y>
- Di Giuseppe F, Ferranti L, Di Napoli C (2017) The August 2017 heat wave in southern Europe ECMWF. <https://www.ecmwf.int/en/newsletter/153/news/august-2017-heat-wave-southern-europe>
- ENVI (2009) Atmospheric correction module. QUAC and FLAASH user's guide, Version 4.7. ITT Visual Information Solutions, Boulder, CO
- Felde GW, Anderson GP, Cooley TW, Matthew MW, Adler-Golden SM, Berk A, Lee J (2003) Analysis of hyperion data with the FLAASH atmospheric correction algorithm. International Geoscience and Remote Sensing Symposium. Proceedings (IEEE Cat. No.03CH37477), vol 1. pp 90–92
- Frank D, Reichstein M, Bahn M, Thonicke K, Frank D, Mahecha MD, Smith P, van der Velde M, Vicca S, Babst F, Beer C, Buchmann N, Canadell JG, Ciais P, Cramer W, Ibrom A, Miglietta F, Poulter B, Rammig A, Seneviratne SI, Walz A, Wattenbach M, Zavala MA, Zscheischler J (2015) Effects of climate extremes on the terrestrial carbon cycle: concepts, processes and potential future impacts. *Glob Change Biol* 21:2861–2880. <https://doi.org/10.1111/gcb.12916>
- Garcia RA, Cabeza M, Rahbek C, Araújo MB (2014) Multiple dimensions of climate change and their implications for biodiversity. *Science* 344(6183):1247579
- Gu L, Hanson P, Mac Post W, Kaiser D, Yang B, Nemani R, Pallardy S, Meyers T (2008) The 2007 eastern US spring freezes: increased cold damage in a warming world? *Bioscience* 58:253–262
- Hayes DJ, Sader SA (2001) Comparison of change-detection techniques for monitoring tropical forest clearing and vegetation regrowth in a time series. *Photogramm Eng Remote Sens* 67:1067–1075
- Hastie T, Tibshirani R (1990) Generalized additive models. Chapman and Hall/CRC, London
- Houston DT, de Rigo D, Caudullo G (2016) *Fagus sylvatica* and other beeches in Europe: distribution, habitat, usage and threats. In: San-Miguel-Ayanz J, de Rigo D, Caudullo G, Houston Durrant T, Mauri A (eds) European Atlas of Forest Tree Species. Publ. Off. EU, Luxembourg, p e012b90+
- Hufkens K, Friedl MA, Keenan TF, Sonnentag O, Bailey A, O'keefe J et al (2012) Ecological impacts of a widespread frost event following early spring leaf-out. *Glob Change Biol* 18:2365–2377. <https://doi.org/10.1111/J.1365-2486.2012.02712.X>
- IPCC (2014) Climate change 2014: synthesis report. In: Core writing team, Pachauri RK, Meyer LA (eds) Contribution of working groups I, II and III to the fifth assessment report of the intergovernmental panel on climate change. IPCC, Geneva 151 pp
- Jeong SJ, Ho CH, Gim HJ, Brown ME (2011) Phenology shifts at start vs. end of growing season in temperate vegetation over the northern hemisphere for the period 1982–2008. *Glob Change Biol* 17:2385–2399. <https://doi.org/10.1111/j.1365-2486.2011.02397.x>
- Jump AS, Hunt JM, Penuelas J (2006) Rapid climate change-related growth decline at the southern range edge of *Fagus sylvatica*. *Glob Change Biol* 12:2163–2174
- Kim Y, Kimball JS, Didan K, Henebry GM (2014) Response of vegetation growth and productivity to spring climate indicators in the conterminous United States derived from satellite remote sensing data fusion. *Agric For Meteorol* 194:132–143. <https://doi.org/10.1016/j.agrformet.2014.04.001>
- Kovalskyy V, Roy DP, Zhang XY, Ju J (2012) The suitability of multi-temporal web-enabled Landsat data NDVI for phenological monitoring – a comparison with flux tower and MODIS NDVI. *Remote Sens Lett* 3(4):325–334. <https://doi.org/10.1080/01431161.2011.593581>
- Kramer PJ, Kozlowski TT (1979) Physiology of Woody plants. Academic Press, New York
- Kramer K, Leinonen I, Loustau D (2000) The importance of phenology for the evaluation of impact of climate change on growth of boreal, temperate and Mediterranean forests ecosystems: an overview. *Int J Biometeorol* 44:67–75
- Kreyling J, Thiel D, Nagy L, Jentsch A, Huber G, Konnert M, Beierkuhnlein C (2012) Late frost sensitivity of juvenile *Fagus sylvatica* L. differs between southern Germany and Bulgaria and depends on preceding air temperature. *Eur J Forest Res* 131(3):717–725
- Lindner M, Fitzgerald JB, Zimmermann NE, Reyer C, Delzon S, van der Maaten E, Schelhaas MJ, Lasch P, Eggers J, van der Maaten-Theunissen M, Suckow F, Psomas A, Poulter B, Hanewinkel M (2014) Climate change and European forests: what do we know, what are the uncertainties, and what are the implications for forest management? *J Environ Manag* 146:69–83. ISSN 0301-4797. <https://doi.org/10.1016/j.jenvman.2014.07.030>
- Lu D, Mausel P, Brondizio E, Moran E (2004) Change detection techniques. *Int J Remote Sens* 25:2365–2407
- Lunetta RS, Knight JF, Ediriwickrema J, Lyon JG, Worthy LD (2006) Land-cover change detection using multi-temporal MODIS NDVI data. *Remote Sens Environ* 105:142–154. <https://doi.org/10.1016/j.rse.2006.06.018>
- Lyon JG, Yuan D, Lunetta RS, Elvidge CD (1998) A change detection experiment using vegetation indices. *Photogramm Eng Remote Sens* 64(2):143–150
- Mancino G, Nolè A, Ripullone F, Ferrara A (2014) Landsat TM imagery and NDVI differencing to detect vegetation change: assessing natural forest expansion in Basilicata, southern Italy. *iForest* 7:75–84
- Menzel A, Helm R, Zang C (2015) Patterns of late spring frost leaf damage and recovery in a European beech (*Fagus sylvatica* L.) stand in South-Eastern Germany based on repeated digital photographs. *Front Plant Sci* 6:110. <https://doi.org/10.3389/fpls.2015.00110>
- Ministero dell'Ambiente e della Tutela del Territorio e del Mare – Geoportale nazionale (2012) Modello digitale del terreno (DTM), 20, metri. <http://www.pcn.minambiente.it/GN/>
- Nabuurs GJ, Masera O, Andrasko K, Benitez-Ponce P, Boer R, Dutschke M, Elsiddig E, Ford-Robertson J, Frumhoff P, Karjalainen T, Krankina O, Kurz WA, Matsumoto M, Oyhantcabal W, Ravindranath NH, Sanz Sanchez MJ, Zhang X (2007) Forestry. In: Metz B, Davidson OR, Bosch PR, Dave R, Meyer LA (eds) Climate change 2007: mitigation, Contribution of Working Group III to the 4th Assessment Report of the IPCC. Cambridge University Press, Cambridge
- Nolè A, Rita A, Ferrara A, Borghetti M (2018) data_sheet_nole_et_al.txt. V1. Figshare. [Dataset] <https://doi.org/10.6084/m9.figshare.6409235.v1>
- Nicholls N, Alexander L (2007) Has the climate become more variable or extreme? *Progress* 1992-2006. *Progr Phys Geogr* 31:77–87
- Pagter M, Arora R (2013) Winter survival and deacclimation of perennials under warming climate: physiological perspectives. *Physiol Plant* 147:75–87. <https://doi.org/10.1111/j.1399-3054.2012.01650x>
- Pan Y, Birdsey RA, Fang J, Houghton R, Kauppi PE, Kurz WA, Phillips OL, Shvidenko A, Lewis SL, Canadell JG, Ciais P, Jackson RB, Pacala SW, McGuire AD, Piao S, Rautiainen A, Sitch S, Hayes D (2011) A large and persistent carbon sink in the world's forests. *Science* 333:988–993. <https://doi.org/10.1126/science.1201609>

- Pasquarella VJ, Holden CE, Kaufman L, Woodcock CE (2016) From imagery to ecology: leveraging time series of all available Landsat observations to map and monitor ecosystem state and dynamics. *Remote Sens Ecol Conserv* 2:152–170. <https://doi.org/10.1002/rse224>
- Podeh SS, Oladi J, Pormajidian MR, Zadeh MM (2009) Forest change detection in the north of Iran using TM/ETM+ imagery. *Asian J Appl Sci* 2:464–474. <https://doi.org/10.3923/ajaps2009464474>
- Príncipe A, van der Maaten E, van der Maaten-Theunissen M, Struwe T, Wilmking M, Kreyling J (2017) Low resistance but high resilience in growth of a major deciduous forest tree (*Fagus sylvatica* L.) in response to late spring frost in southern Germany. *Trees* 31(2):743–751. <https://doi.org/10.1007/s00468-016-1505-3>
- Pu R, Gong P, Tian Y, Miao X, Carruthers RI, Anderson GL (2008) Invasive species change detection using artificial neural networks and CASI hyperspectral imagery. *Environ Monit Assess* 140(1-3): 15–32. <https://doi.org/10.1007/s10661-007-9843-7>
- Rigby JR, Porporato A (2008) Spring frost risk in a changing climate. *Geophys Res Lett* 35:L12703. <https://doi.org/10.1029/2008GL033955>
- Roy DP, Wulder MA, Loveland TR, Woodcock CE, Allen RG, Anderson MC, Helder D, Irons JR, Johnson DM, Kennedy R, Scambos TA, Schaaf CB, Schott JR, Sheng Y, Vermote EF, Belward AS, Bindschadler R, Cohen WB, Gao F, Hipple JD, Hostert P, Huntington J, Justice CO, Kilic A, Kovalsky V, Lee ZP, Lyburner L, Masek JG, McCorkel J, Shuai Y, Trezza R, Vogelmann J, Wynne R, Zhu Z (2014) Landsat-8: science and product vision for terrestrial global change research. *Remote Sens Environ* 145:154–172
- Sakai A, Larcher W (1987) Frost survival of plants responses and adaptation to freezing stress. Springer-Verlag, Berlin
- Schowengerdt RA (1997) Remote sensing models and methods for image processing, 2nd edn. Academic, New York, 525 p
- Visnjic C, Dohrenbusch A (2004) Frostresistenz und Phänologie europäischer Buchenprovenienzen. *Allg Forst Jagdztg* 175:101–108
- Vitasse Y, Lenz A, Körner C (2014) The interaction between freezing tolerance and phenology in temperate deciduous trees. *Front Plant Sci* 5:541. <https://doi.org/10.3389/fpls201400541>
- Vitasse Y, Bresson C, Kremer A, Michalet R, Delzon S (2010) Quantifying phenological plasticity to temperature in two temperate tree species. *Funct Ecol* 24(6):1211–1218. <https://doi.org/10.1111/j.1365-2435.2010.01748.x>
- Vitasse Y, Schneider L, Rixen C, Christen D, Rebetez M (2018) Increase in the risk of exposure of forest and fruit trees to spring frosts at higher elevations in Switzerland over the last four decades. *Agr Forest Meteorol* 248:60–69. <https://doi.org/10.1016/j.agrformet.2017.09.005>
- Zhang X, Friedl MA, Schaaf CB, Strahler AH, Hodges JCF, Gao F, Reed BC, Huete A (2003) Monitoring vegetation phenology using MODIS. *Remote Sens Environ* 84:471–475
- Zhang X, Friedl MA, Schaaf CB, Strahler AH (2004) Climate controls on vegetation phenological patterns in northern mid- and high latitudes inferred from MODIS data. *Glob Chang Biol* 10:1133–1145. <https://doi.org/10.1111/j.1365-2486.2004.00784.x>
- Wang T, Otle C, Peng S, Janssens IA, Lin X, Poulter B, Yue C, Ciais P (2014) The influence of local spring temperature variance on 452 temperature sensitivity of spring phenology. *Glob Chang Biol* 20: 1473–1480. <https://doi.org/10.1111/gcb.12509>
- White K, Pontius J, Schaberg P (2014) Remote sensing of spring phenology in northeastern forests: a comparison of methods, field metrics and sources of uncertainty. *Remote Sens Environ* 148:97–107. <https://doi.org/10.1016/j.rse.2014.03.017>
- Williams CA (2014) Heat and drought extremes likely to stress ecosystem productivity equally or more in a warmer, CO² rich future. *Environ Res Lett* 9(10):6224–6229
- Williams IN, Torn MS, Riley WJ, Wehner MF (2014) Impacts of climate extremes on gross primary production under global warming. *Environ Res Lett* 9(9):101002
- Wilson EH, Sader SA (2002) Detection of forest harvest type using multiple dates of Landsat TM imagery. *Remote Sens Environ* 80:385–396. [https://doi.org/10.1016/S0034-4257\(01\)00318-2](https://doi.org/10.1016/S0034-4257(01)00318-2)
- Wood S (2006) Generalized additive models: an introduction with R. Chapman and Hall/CRC, Boca Raton, FL, pp 391
- Xie Y, Wang X, Silander JA (2015) Deciduous forest responses to temperature, precipitation, and drought imply complex climate change impacts. *PNAS* 112:13585–13590. <https://doi.org/10.1073/pnas.1509991112>